The Value of Radiomic Features of Primary Breast Tumor in STIR Sequences in Predicting Axilla Metastasis

Günay Rona*[a], Meral Arifoğlu[a], Ahmet Tekin Serel[b], Tamer Baysal[a]

[a]*Department of Radiology, Kartal Doktor Lütfi Kırdar Training and Research Hospital, University of Health Sciences, Istanbul, Turkey*

[b]*Department of Urology, Suleyman Demirel University School of Medicine, Istanbul, Turkey*

ARTICLE INFO

ABSTRACT

Background: Detection of axillary metastases in breast cancer is critical for treatment options and prognosis. The aim of this study is to investigate the value of radiomic features obtained from short tau inversion recovery (STIR) sequences in magnetic resonance imaging (MRI) of primary tumor in breast cancer in predicting axillary lymph node metastasis (ALNM).

Methods: Lesions of 165 patients with a mean age of 51.12 ±11 (range 28-82) with newly diagnosed invasive breast cancer who underwent breast MRI before treatment were manually segmented from STIR sequences in the 3D Slicer program in all sections. Machine learning (ML) analysis was performed using the extracted 851 features Python 3.11, Pycaret library program. Datasets were randomly divided into train (123, 80%) and independent test (63, 20%) datasets. The performances of ML algorithms were compared with area under curve (AUC), accuracy, recall, presicion and F1 scores.

Results: Accuracy and AUC in the training set were in the range of 57 %-86 % and 0.50-0.95, respectively. The best model in the training set was the catBoost classifier with an AUC of 0.95 and 84% accuracy. The AUC, accuracy, recall, precision values and F1 score of the CatBoost classifier on the test set were 0.92, 84 %, 89 %, 85 %, 86 %, respectively.

Conclusion: Radiomic features obtained from primary tumors on STIR sequences have the potential to predict ALNM in invasive breast cancer.

INTRODUCTION

Axillary lymph node metastasis (ALNM) is one of the most important prognostic factors determining survival in breast cancer.[1] The status of the axilla determines the need for axillary lymph node dissection (ALND), axillary radiotherapy, neoadjuvant or adjuvant chemotherapy.[2] Accurate determination of the axillary status before treatment is critical in determining individualized treatment options.[3] Age, tumor size, tumor quadrant, multifocality, histological grade, pathological type, receptor status, molecular subtype are associated with ALNM.[4-9]

Radiomic analysis aims to contribute to diagnosis, treatment and follow-up processes by extracting specific quantitative information about diseases that the human eye cannot perceive from medical images. With radiomic analysis, the aim is to maximize the information obtained from images by obtaining quantitative data about signal intensities and spatial distribution of inter-pixel relationships. [10]

Recently, radiomics has attracted considerable attention in the medical field, especially in oncology.

*****Address for correspondence:**
Günay Rona, MD,
Cevizli Neighbourhood, Semsi Denizer Road. E-5 Highway District, 34890 Kartal, İstanbul/Turkey
Tel +902164583000
Email: gunayrona@gmail.com

Successful results were also obtained in the diagnosis, treatment and classification of breast cancer. [11] Also, promising results were acquired in the differentiation of malignant and benign breast masses, in the estimation of the grade and receptor status and subtypes of malignant tumors using radiomic features extracted from magnetic resonance imaging (MRI). This method is also promising in the prediction of neoadjuvant chemotherapy response in breast cancer. In studies performed with MRI, it was found that radiomics successfully helped even in the prediction of recurrence of breast cancer. [12-16]

Radiomics features of axillary lymph nodes from T2W MR images were not successful in predicting ALNM. [17] However, ALNM could be predicted with radiomic features obtained from T2-weighted (T2W), diffusion-weighted (DW) and T1+C images of the primary tumor. [18-24]

Our aim in this study was to investigate the performance of radiomic features obtained from short tau inversion recovery (STIR) sequences of primary tumor in predicting axillary metastasis.

METHODS
Participans
Patients diagnosed with invasive breast cancer by core biopsy between August 2017 and February 2023 were evaluated retrospectively. Patients who underwent sentinel lymph node biopsy (SLNB) or ALND and patients who underwent MRI before treatment were included in the study. Patients who received neoadjuvant chemotherapy, or had unknown pathology, another malignancy, a recurrent disease, or artifacts in MRI images were excluded from the study.

MRI Acquisition Protocol
MRI examinations were performed with a 1.5 T MRI device (Philips Ingenia, Philips Healthcare, Best, The Netherlands) using a dedicated 16-channel phased array breast coil. Non-fat-saturated turbo-spin-echo T1 (Field of View (FOV: 302x302 mm, Matrix: 199x203, Flip Angle (FA): 90 deg, Repetition Time (TR): 547 ms, Echo Time (TE): 8 ms, Slice thickness: 3.00 mm, Slice gap: 3.30), spin-echo STIR (FOV: 341x341 mm, Matrix: 263x223, FA: 90 deg, TR: 4040 ms, TE: 65/175.000 ms, Slice thickness: 3.00 mm, Slice gap: 3.30), three dimensional fat-saturated ultrafast spoiled gradient-echo dynamic (FOV: 342x342 mm, Matrix: 342x340, FA: 10 deg, TR: 5 ms, TE: 3 ms, Slice thickness: 2 mm, Slice gap: 1 mm) images were obtained. Dynamic sequences were acquired at 90, 142, 194, 246, and 298 seconds after contrast injection. A single dose of 0.1 mmol/kg body weight gadolinium chelate was administered to the patients with an automatic injector.

Segmentation and Feature Extraction
STIR sequences in DCOM format were transferred to the 3D Slicer program (version 4.10.2; https://www.slicer.org). Resampled images (size:1x1x1 mm) were acquired and normalized. Manual segmentation was performed independently by two radiologists with 8 and 10 years of experience in breast imaging, blinded to the axillary condition of the patients. Segmentation was performed from all axial STIR sequences with tumor. A total of 851 texture features, including first-order, second-order and wavelet-based features were extracted with Slicer-Radiomics (PyRadiomics v3.0.1) (Figure 1). One month later, 30 randomly selected patients were independently segmented by the same two radiologists and radiomic features were extracted again. Thus, interobserver agreement was evaluated.
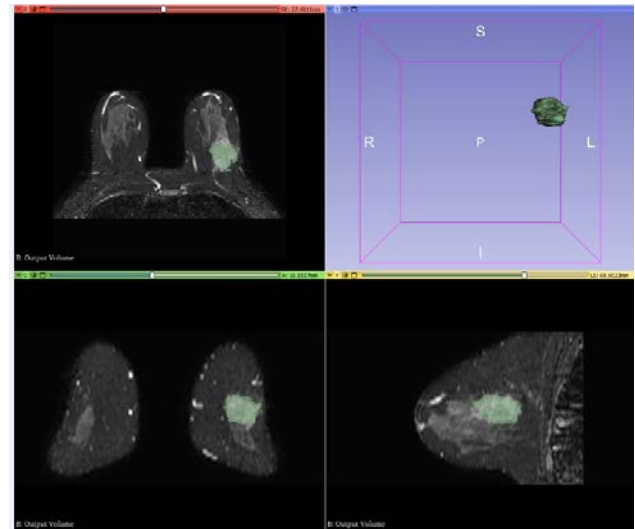
Figure 1. Workflow for extraction of radiomic features from STIR sequences and machine learning analysis

Machine Learning Analysis
Python 3.11 (Jupyter Notebook, Pycaret Library) was used for data processing and machine learning analysis. The synthetic minority oversampling technique (SMOTE) was used to avoid imbalanced data sets. Data normalization was performed before model develepment.

The data sets were randomly divided into training and independent testing sets. We used 10-fold cross validation of the trained models to avoid data overfitting.

Overall, 15 machine learning (ML) algorithms were used. The area under the curve (AUC), accuracy, recall, precision and F1 scores were compared with the performances of the ML algorithms. The best model for accuracy and AUC was selected and evaluated on the test set. AUC, accuracy, recall, precision, and F1 scores were given

by the confusion matrix. The best model was tuned and finalized.

Statistical Analysis

The data were analyzed by the Statistical Package for Social Sciences (SPSS) version 25.0.0.0 software (IBM Corp., Armonk, N.Y., USA). Percentage, mean, and standard deviation were used to present descriptive results. The one-sample Kolmogorov–Smirnov test was used to see if the groups have a normal distribution. Continuous variables with a normal distribution were shown as mean (± standard deviation [SD]). Interobserver agreement was evaluated using ICC values. Features with an ICC value >0.7 were further checked with ML.

RESULTS

In this study, 421 patients were evaluated retrospectively. Overall, 106 patients who did not undergo MRI before treatment, 48 patients whose SLNB or ALND data were not available, 52 patients who received neoadjuvant chemotherapy, 6 patients with recurrent disease, 3 patients with concurrent malignancy and 41 patients with artifacts were excluded from the study. Thus, 165 patients with a mean age of 51.12 ±11 (range 28-82) were included in the study. While 92 (55.76 %) patients had axillary metastases, 73 (44.24 %) did not have axillary metastases. The mean lesion size was 24.78 ± 15 (6-120) mm.

Altogether, 667 features with ICC values above 0.7 were evaluated with ML. Wavelet filtered texture features, maximum 3D diameter, skewness kurtosis and maximum signal features showed a high correlation with ALNM. The features selected by ML algorithms and their importance are presented in Figure 2.

The accuracy and AUC of ML algorithms on the training set were in the range of 57%-86% and 0.50-0.95, respectively (Table 1). Among the ML algorithms, the best model was CatBoost classifier (AUC:0.95, accuracy: 84%). The ROC curve showing the success of the CatBoost classifier in predicting ALNM is presented in Figure 3.
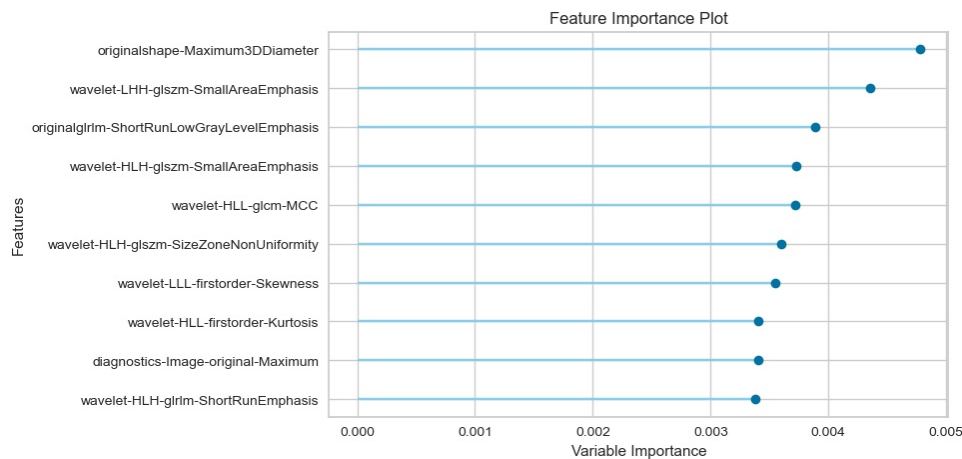
Figure 2. The features selected by the ML algorithms

Table 1. Performance of machine learning models in differentiating those with axillary metastases from those without axillary metastases in patients with invasive breast cancer in the training set from STIR sequences.

Model	Accuracy	AUC	Recall	Prec.	F1
CatBoost Classifier	0.8391	0.9518	0.9288	0.8197	0.8675
Extra Trees Classifier	0.8391	0.9517	0.8981	0.8326	0.8618
Light Gradient Boosting Machine	0.8696	0.9510	0.9212	0.8632	0.8870
Gradient Boosting Classifier	0.8652	0.9480	0.9058	0.8687	0.8834
Random Forest Classifier	0.8522	0.9461	0.9058	0.8447	0.8720
Extreme Gradient Boosting	0.8652	0.9379	0.9141	0.8626	0.8842
Ada Boost Classifier	0.8261	0.8644	0.8679	0.8406	0.8480
Logistic Regression	0.8174	0.8479	0.8372	0.8478	0.8299
Quadratic Discriminant Analysis	0.8261	0.8427	0.7045	0.9798	0.8091
Decision Tree Classifier	0.8348	0.8338	0.8449	0.8654	0.8479
Linear Discriminant Analysis	0.7696	0.7738	0.7660	0.8083	0.7820
K Neighbors Classifier	0.7435	0.7348	0.8263	0.7443	0.7815
Naive Bayes	0.5739	0.5393	0.8641	0.5767	0.6897
Dummy Classifier	0.5565	0.5000	1.0000	0.5565	0.7149
SVM - Linear Kernel	0.7696	0.0000	0.7814	0.8094	0.7856
Ridge Classifier	0.7957	0.0000	0.8212	0.8274	0.8116
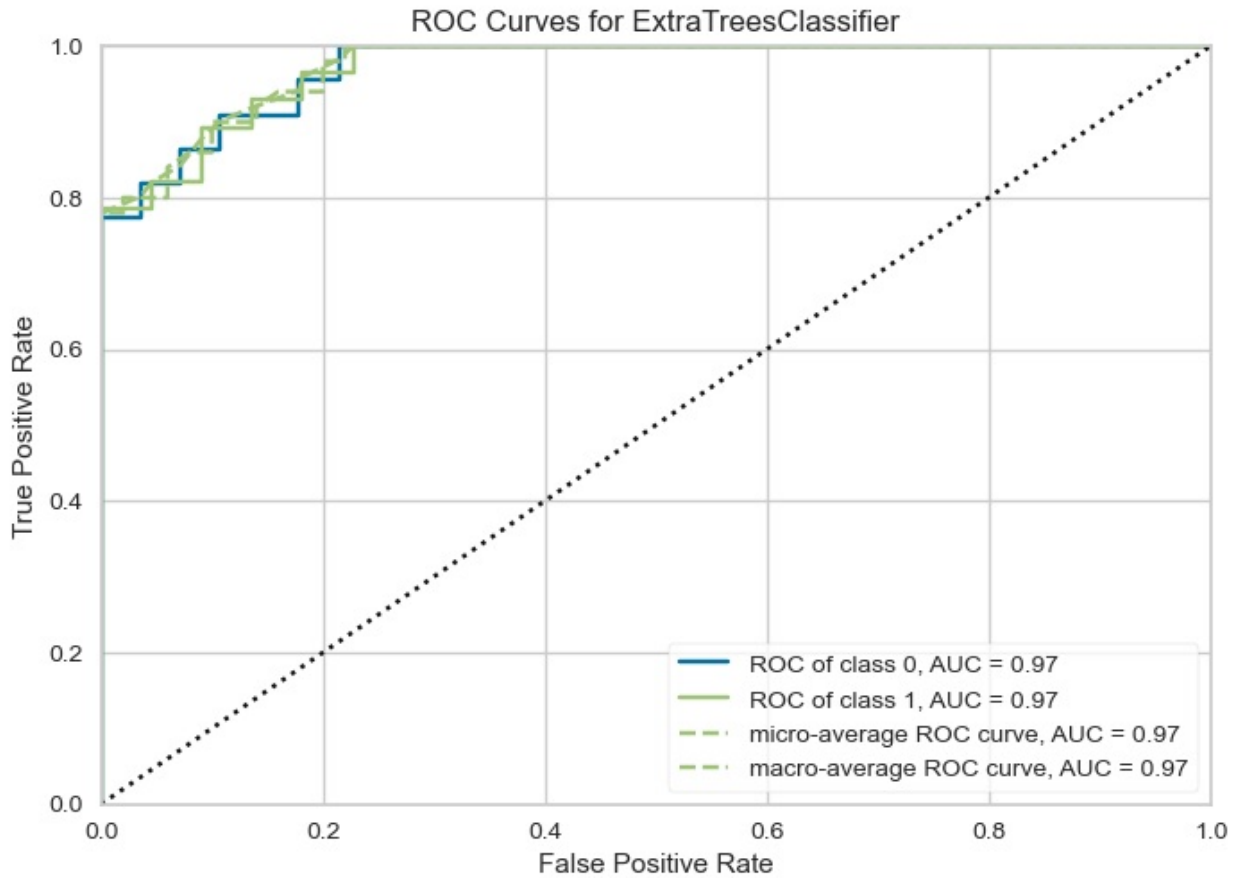
Figure 3. Receiver operating characteristics curve of the CatBoost classifier in predicting axillary lymph node metastasis.

CatBoost classifier was evaluated on the test set. After tuning the AUC, accuracy, recall and precision values and F1 score were 0.92, 84 %, 89 %, 85 %, 86 %, respectively. The CatBoost classifier model had a 92.86% sensitivity and 86.36 % specificity in detecting ALNM. The classification report and confusion matrix showing the performance of the CatBoost model are presented in Figure 4.
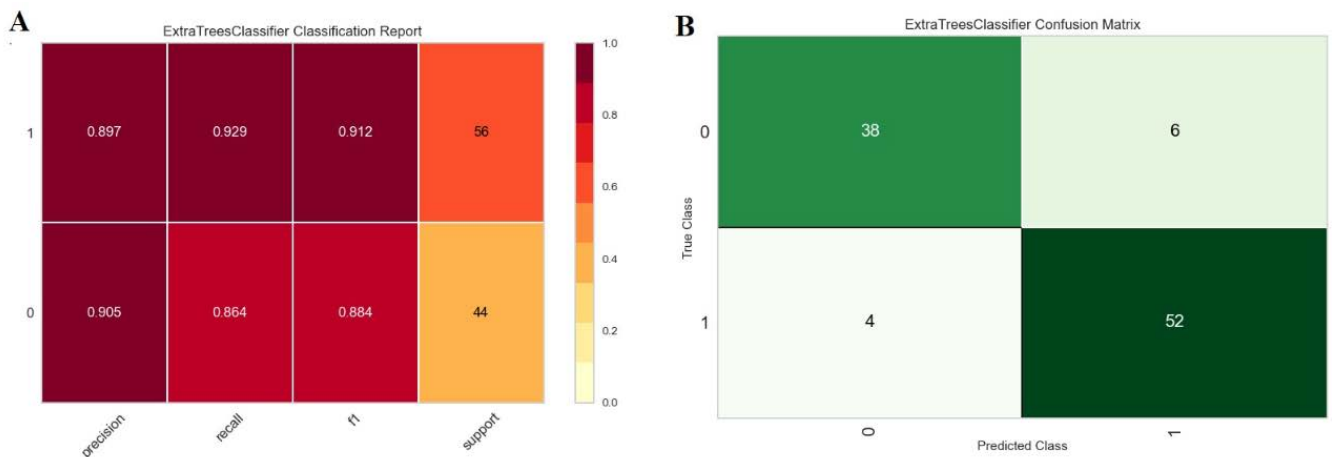
Figure 4. Confusion matrix (A), classification report (B) for CatBoost classifier in predicting axillary lymph node metastasis.

DISCUSSION

Recently, less invasive treatment approaches for the axilla have been accepted. SLNB is preferred instead of ALND in early stage breast cancer. Determining the condition of the axilla in the preoperative period is important in the development of surgical plans. For individualized and minimally invasive treatment options, it is important to determine the condition of the axilla before treatment. [25] Among the imaging methods, ultrasound (US) is the primary tool in the evaluation of the axilla.

However, approximately 15-20% of patients with negative US findings have metastases in the SLNB. In mammography (MG), 50% of level 1 axillary lymph nodes can be visualized and levels 2 and 3 cannot be evaluated. [26] It has been reported that MRI has similar sensitivity to US, but less specificity in detecting nodal metastases. [27]

In previous studies, ALNM could be predicted by the radiomics features of the primary tumor in MRI. Yu *et al.*, on the other hand, successfully predicted axillary lymph node status on T1+C, T2W, DW MRI with a multiomic signature including radiomics features and clinicopathologic features obtained from lymph nodes and primary tumor. [19] Qiu *et al.* were successful in predicting ALNM using clinicopathological features, morphological features of lymph nodes from MR images, and radiomics features of the primary mass. Radiomic features obtained from DWI, T2W and T1+C images of the primary mass were successful in predicting ALNM with an AUC value of 0.806. [20] Wang *et al.* were able to predict axillary metastases with an AUC value of over 0.80 with the radiomics and deep learning features obtained from dynamic contrast-enhanced (DCE) MRI. [21] Chen *et al.* were able to predict ALNM with the nomogram created by the radiomics and clinicopathological features of the primary tumor obtained from DW and DCE MRI (AUC value in the training set and test set, respectively 0.80, 0.71). [22] Using DCE MRI, Liu and colleagues were able to predict ALNM by tumoral and peritumoral radiomics signature (AUC values in the training and test set were 0.872, 0.863, respectively). [23] Cui *et al.* predicted axillary lymph node status with radiomic features obtained from second post-contrast images on MRI with an AUC of 0.86 and an accuracy of 89%. [24] However, none of these studies presented the performance of T2W images alone in predicting ALNM.

Dong and colleagues were successful in predicting sentinel lymph node metastasis with radiomic features obtained from fat-suppressed T2W and DW MRI images. With T2W alone, AUC values were 0.847 in the training set and 0.770 in the validation set. With DW MRI, they obtained AUC values of 0.847 in the training set and 0.787 in the validation set. When they combined the features obtained from T2W and DW images, the AUC values were 0.863 in the training set and 0.805 in the validation set. [18]

In our study, we predicted ALNM with 0.92 AUC and 84% accuracy in the training and validation set with the radiomic features obtained from STIR sequences by modeling using machine learning analysis. The ML models used except Naive Bayes, Dummy Classifier, SVM - Linear Kernel and Ridge Classifier showed successful performance with at least 0.73 AUC and 74 % accuracy. CatBoost Classifier, Extra Trees Classifier, Light Gradient Boosting Machine, Gradient Boosting Classifier and Extreme Gradient Boosting had AUC values above 0.93 and accuarrcy values above 86 %. Among the models CatBoost Classifier, Extra Trees Classifier, Light Gradient Boosting, Gradient Boosting Classifier and Random Forest Classifier had the highest performance with 0.95 AUC values and with 84-86 % accurracy values. Among these models, CatBoost Classifier had the highest recall and precision values with 0.93 and 82 %, respectively.

Radiomics features derived from T2W sequences detected ALNM with an AUC of up to 0.85. When DWI and DCE were combined with T2W, the AUC value increased to 0.86.[18] In our study, only STIR arrays reached 0.92 AUC. Since STIR sequences are used in routine breast MRI in some centers, they may contribute to the prediction of ALNM. To our knowledge, STIR radiomics have not been used in studies investigating ALNM. STIR sequences stand out compared to other fat suppression techniques by providing more uniform fat suppression without being affected by magnetic field inhomogeneity. Although the signal-to-noise ratio is poor, it is useful because it includes both T1 and T2 contrast.

There is a correlation between tumor size and lymph node metastasis. [9] In our study, the maximum diameter of the tumor and axillary metastases showed a high correlation. Kurtosis and skewness features, which evaluate intralesional homogenetiy, were also correlated with ALNM.

Our study has some limitations. Its retrospective nature, small number of patients, and choosing the largest lesion in patients with more than one lesion are among the limitations of our study. Another limitation is that we did not divide the patients according to the number of metastatic lymph nodes.

CONCLUSION

In conclusion, radiomic features obtained from the primary tumor on STIR sequences have the potential to predict ALNM. STIR sequences are noninvasive and are currently used as a routine component of breast MRI in some centers. However, some lesions cannot be segmented since they have signal intensity close to parchyma in STIR sequences.

ETHICAL CONSIDERATIONS

Ethics committee approval was obtained from our institution for this retrospective study (Approve no: 202351425036).

CONFLICT OF INTEREST

ACKNOWLEDGEMENTS

REFERENCES

1. Beenken SW, Urist MM, Zhang Y, Desmond R, Krontiras H, Medina H, et al. Axillary lymph node status, but not tumor size, predicts locoregional recurrence and overall survival after mastectomy for breast cancer. *Ann Surg* 2003;237:732-739. doi: 10.1097/01.SLA.0000065289.06765.71.

2. Rao R, Euhus D, Mayo HG, Balch C. Axillary node interventions in breast cancer: a systematic review. *JAMA* 2013;310:1385-1394.doi: 10.1001/jama.2013.277804.

3. Diessner J, Anders L, Herbert S, Kiesel M, Bley T, Schlaiss T, et al. Evaluation of different imaging modalities for axillary lymph node staging in breast cancer patients to provide a personalized and optimized therapy algorithm. *J Cancer Res Clin Oncol.* 2023 Jul;149(7):3457-3467. doi: 10.1007/s00432-022-04221-9.

4. Chua B, Ung O, Taylor R, Boyages J. Frequency and predictors of axillary lymph node metastases in invasive breast cancer. *ANZ J Surg*. 2001 Dec;71(12):723-8. doi: 10.1046/j.1445-1433.2001.02266.x.

5. Van Zee KJ, Manasseh DM, Bevilacqua JL, Boolbol SK, Fey JV, Tan LK, et al. A nomogram for predicting the likelihood of additional nodal metastases in breast cancer patients with a positive sentinel node biopsy. *Ann Surg Oncol*. 2003 Dec;10(10):1140-51. doi: 10.1245/aso.2003.03.015.

6. Zhang J, Li X, Huang R, Feng WL, Kong YN, Xu F, et al. A nomogram to predict the probability of axillary lymph node metastasis in female patients with breast cancer in China: A nationwide, multicenter, 10-year epidemiological study. *Oncotarget* 2017;8:35311-35325. doi: 10.18632/oncotarget.13330.

7. Cutuli B, Velten M, Martin C. Assessment of axillary lymph node involvement in small breast cancer: analysis of 893 cases. *Clin Breast Cancer* 2001;2:59-66. doi: 10.3816/CBC.2001.n.012.

8. Andea AA, Bouwman D, Wallis T, Visscher DW. Correlation of tumor volume and surface area with lymph node status in patients with multifocal/multicentric breast carcinoma. *Cancer* 2004;100:20-27. doi: 10.1002/cncr.11880.

9. Chen W, Wang C, Fu F, Yang B, Chen C, Sun Y. A Model to Predict the Risk of Lymph Node Metastasis in Breast Cancer Based on Clinicopathological Characteristics. *Cancer Manag Res* 2020;12:10439-10447. doi: 10.2147/CMAR.S272420.

10. Van Timmeren JE, Cester D, Tanadini-Lang S, Alkadhi H, Baessler B. Radiomics in medical imaging-"how-to" guide and critical reflection. Insights *Imaging* 2020;11:91. doi: 10.1186/s13244-020-00887-2.

11. Conti A, Duggento A, Indovina I, Guerrisi M, Toschi N. Radiomics in breast cancer classification and prediction. *Semin Cancer Biol* 2021;72:238-250. doi: 10.1016/j.semcancer.2020.04.002.

12. Parekh VS, Jacobs MA. Integrated radiomic framework for breast cancer and tumor biology using advanced machine learning and multiparametric. *MRI NPJ Breast Cancer* 2017;3:43. doi: 10.1038/s41523-017-0045-3.

13. Whitney HM, Taylor NS, Drukker K, Edwards AV, Papaioannou J, Schacht D,et al. Additive Benefit of Radiomics Over Size Alone in the Distinction Between Benign Lesions and Luminal A Cancers on a Large Clinical Breast MRI Dataset. Acad *Radiol*. 2019;26:202-209. doi: 10.1016/j.acra.2018.04.019.

14. Bickelhaupt S, Paech D, Kickingereder P, Steudle F, Lederer W, Daniel H, et al. Prediction of malignancy by a radiomic signature from contrast agent-free diffusion MRI in suspicious breast lesions found on screening mammography. J Magn Reson *Imaging* 2017;46:604-616. doi: 10.1002/jmri.25606.

15. Bickelhaupt S, Jaeger PF, Laun FB, Lederer W, Daniel H, Kuder TA, et al. Radiomics Based on Adapted Diffusion Kurtosis Imaging Helps to Clarify Most Mammographic Findings Suspicious for Cancer. *Radiology* 2018;287:761-770. doi: 10.1148/radiol.2017170273.

16. Antropova N, Huynh BQ, Giger ML. A deep feature fusion methodology for breast cancer diagnosis demonstrated on three imaging modality datasets. *Med Phys* 2017;44:5162-5171. doi: 10.1002/mp.12453.

17. Samiei S, Granzier RWY, Ibrahim A, Primakov S, Lobbes MBI, Beets-Tan RGH, et al. Dedicated Axillary MRI-Based Radiomics Analysis for the Prediction of Axillary Lymph Node Metastasis in Breast Cancer. *Cancers (Basel)* 2021 12;13:757. doi: 10.3390/cancers13040757.

18. Dong Y, Feng Q, Yang W, Lu Z, Deng C, Zhang L, et al. Preoperative prediction of sentinel lymph node metastasis in breast cancer based on radiomics of T2-weighted fat-suppression and diffusion-weighted MRI. *Eur Radiol*. 2018;28:582-591. doi: 10.1007/s00330-017-5005-7.

19. Yu Y, He Z, Ouyang J, Tan Y, Chen Y, Gu Y, et al. Magnetic resonance imaging radiomics predicts preoperative axillary lymph node metastasis to support surgical decisions and is associated with tumor microenvironment in invasive breast cancer: A machine learning, multicenter study. *EBioMedicine* 2021;69:103460. doi: 10.1016/j.ebiom.2021.103460.

20. Qiu Y, Zhang X, Wu Z, Wu S, Yang Z, Wang D, et al. MRI-Based Radiomics Nomogram: Prediction of Axillary Non-Sentinel Lymph Node Metastasis in Patients With Sentinel Lymph Node-Positive Breast Cancer. *Front Oncol* 2022;12:811347. doi: 10.3389/fonc.2022.811347.

21. Wang D, Hu Y, Zhan C, Zhang Q, Wu Y, Ai T. A nomogram based on radiomics signature and deep-

learning signature for preoperative prediction of axillary lymph node metastasis in breast cancer. *Front Oncol* 2022;12:940655. doi: 10.3389/fonc.2022.940655.

22. Chen Y, Wang L, Dong X, Luo R, Ge Y, Liu H, Zhang Y, et al. Deep Learning Radiomics of Preoperative Breast MRI for Prediction of Axillary Lymph Node Metastasis in Breast Cancer. *J Digit Imaging* 2023;1-9. doi: 10.1007/s10278-023-00818-9.

23. Liu Y, Li X, Zhu L, Zhao Z, Wang T, Zhang X, et al. Preoperative Prediction of Axillary Lymph Node Metastasis in Breast Cancer Based on Intratumoral and Peritumoral DCE-MRI Radiomics Nomogram. *Contrast Media Mol Imaging* 2022 18;2022:6729473. doi: 10.1155/2022/6729473.

24. Cui X, Wang N, Zhao Y, Chen S, Li S, Xu M, et al. Preoperative Prediction of Axillary Lymph Node Metastasis in Breast Cancer using Radiomics Features of DCE-MRI. *Sci Rep* 2019;9(1):2240. doi: 10.1038/s41598-019-38502-0.

25. Morrow M. Management of the Node-Positive Axilla in Breast Cancer in 2017: Selecting the Right Option. *JAMA Oncol* 2018;4:250-251. doi: 10.1001/jamaoncol.2017.3625.

26. Chang JM, Leung JWT, Moy L, Ha SM, Moon WK. Axillary Nodal Evaluation in Breast Cancer: *State of the Art. Radiology* 2020;295:500-515. doi: 10.1148/radiol.2020192534.

27. Cooper KL, Meng Y, Harnan S, Ward SE, Fitzgerald P, Papaioannou D, et al. Positron emission tomography (PET) and magnetic resonance imaging (MRI) for the assessment of axillary lymph node metastases in early breast cancer: systematic review and economic evaluation. *Health Technol Assess* 2011;15:iii-134. doi: 10.3310/hta15040.

How to Cite This Article